ELSEVIER

Journal of Power Sources 97–98 (2001) 336–343

JOURNAL OF POWER SOURCES

www.elsevier.com/locate/jpowsour

Synthesis and characterization of $Li_2Mn_4O_9$ cathode material

W.P. Kilroy*, W.A. Ferrando, S. Dallek

Naval Surface Warfare Center, Carderock Division, West Bethesda, MD 20817, USA

Received 11 July 2000; accepted 4 January 2001

Abstract

A highly oxidized lithium manganospinel, $Li_2Mn_4O_{8+z}$, was prepared from $LiMnO_4$ and $MnCO_3$ precursors. The effect of synthesis temperature, time, and oxygen partial pressure on the extent of oxidation of the material was investigated by thermogravimetry (TG). X-ray diffraction (XRD), potentiometric titration, thermogravimetry, and elemental analyses were used to determine the stoichiometry of the product. Published by Elsevier Science B.V.

Keywords: Thermogravimetry; X-ray diffraction; $Li_2Mn_4O_9$

1. Introduction

Lithium manganospinels have been investigated in recent years as lithium insertion cathodes for lithium-ion batteries [1–6]. The difficulty in preparing the fully oxidized material $Li_2Mn_4O_9$, in a reproducible manner, is well known [7]. Strict control of experimental conditions such as temperature, time, particle size of the precursor materials, and oxygen partial pressure is essential for producing fully oxidized, single-phase material. Studies to date, however, show clearly that the fully oxidized $Li_2Mn_4O_9$ phase has never been prepared successfully. The value of z in $Li_2Mn_4O_{8+z}$ has generally been reported to be in the range 0.2 to 0.5 [8–10].

The precursor materials reported in the literature for the solid state synthesis of $Li_2Mn_4O_9$ are usually oxides, hydroxides, carbonates or nitrates of magnesium and lithium. We report here on the synthesis of spinel $Li_2Mn_4O_9$ using a new precursor mixture $LiMnO_4{\cdot}3H_2O$ and $MnCO_3$. The rationale for choosing $LiMnO_4{\cdot}3H_2O$ as one of the precursors was that it forms a melt, which has recently been reported to improve contact among the reactants [11]. The effectiveness of using $LiMnO_4$ as a reagent to prepare layered manganese oxides has also been reported [12].

Our objective was to prepare a highly oxidized cathode spinel material, i.e. to maximize the value of z in $Li_2Mn_4O_{8+z}$, and to characterize the material. Thermogravimetry (TG) was employed to determine the optimal experimental conditions for the synthesis of the cathode and the extent of oxidation of the product. The stoichiometry was determined from potentiometric titration and elemental analysis of Li and Mn. The superior electrochemical behavior of the material was demonstrated using coin cells and single cell tests in hermetically sealed glass laboratory cells.

2. Experimental

2.1. Reagents and material preparation

The lithium manganospinels spinels were prepared by solid-state reactions of stoichiometric amounts of thoroughly mixed powders of $LiMnO_4{\cdot}3H_2O$ (Fisher) and $MnCO_3$ (Aldrich, 99.9%). The reactions were investigated over a temperature range from 275 to 550°C in a quartz tube furnace under flowing oxygen. After the optimal temperature range was established, the effects of heating time, grinding, and oxidizing environment on the synthesis were investigated. The precursors were heated at 5°C/min until the permanganate formed a melt, whereupon the temperature was held constant for about 15 min. Heating was continued until the calcination temperature was reached. The effects of air, oxygen, ozone/oxygen and the addition of 30% hydrogen peroxide under flowing oxygen as oxidizing environments were examined.

2.2. Materials characterization

A TA Instruments, Inc., 951 thermogravimetric analyzer was used in this study. The purity and moisture content of the precursor materials were determined by TG measurements in a helium atmosphere. TG measurements of precursor mixtures in oxygen were used to determine the optimal

* Corresponding author.

0378-7753/01/$ – see front matter. Published by Elsevier Science B.V.
PII: S0378-7753(01)00665-6

temperatures and times for the bulk synthesis of the spinels in a tube furnace. The extent of the oxidation of the spinel was determined by TG weight loss measurements in helium. Fourier transform infrared (FTIR) spectroscopy was used to analyze the evolved gases from the thermal decomposition of the spinel materials, using a Nicolet 510P spectrometer interfaced to the TG instrument with a heated transfer line.

2.3. Chemical analysis

Powder X-ray diffraction (XRD) was used to evaluate the purity of the spinel materials. The composition was determined using direct current argon plasma emission spectroscopy (DCP) in combination with potentiometric titration. Lithium content was determined by DCP. Manganese was determined by potentiometric analysis. The oxygen content was determined from the Li and Mn results. The oxidation state of Mn in the spinel was calculated from analysis of the oxidizing power of Mn and the total manganese. The former was determined by dissolving the spinel in an excess of acidified standard ferrous solution and titrating the remaining Fe^{2+} using standard $KMnO_4$. After addition of excess pyrophosphate to convert Mn^{2+} to Mn^{3+}, total Mn was determined by potentiometric titration with standard $KMnO_4$. The efficacy of the titrimetric procedure was evaluated from analysis of standard $LiMnO_4$ and a standard ore of manganese. The presence of unreacted Mn^{2+} in our material could be detected by comparing the titrimetric results with those found from the addition of known amounts of $MnCO_3$ to standard samples of $LiMn_2O_4$.

2.4. Electrochemical evaluation

The electrochemical behavior of the spinel material was determined in hermetically sealed glass lab cells containing approximately 0.5 in.^{2} electrodes. The lab cell consisted of a cathode sandwiched between two anodes and separated by two layers of Celgard. All components were assembled in a dry room. The electrolyte was either 1 M $LiAsF_6$ in propylene carbonate or 1 M $LiPF_6$ in a 1:1 mixture of ethylene carbonate (EC) and ethylmethylcarbonate (EMC). The anode was lithium foil on nickel exmet. The cathode was prepared by dissolving polyvinylidene fluoride (PVDF) in a minimum amount of dimethylsulfoxide (DMSO), followed by adding a mixture of super-P carbon and the as-synthesized spinel. Additional DMSO was added to form a thick paste.

The composite cathode consisted of spinel, carbon and PVDF in an 88:8:4 to 85:10:5 weight ratio that was pressed onto Al exmet and dried overnight under vacuum at 135°C. The cathode was initially charged, followed by charge–discharge cycling under galvanostatic conditions. This cathode material was also cycled versus a lithium anode in a coin cell using 1 M $LiPF_6$ in electrolyte consisting of a 5:4:1 ratio of ethylene carbonate–dimethylcarbonate–diethylcarbonate, i.e. EC–DMC–DEC.

3. Results and discussion

3.1. Reaction mechanism

A preliminary TG experiment was conducted to determine the sequence of reactions in the synthesis of the $Li_2Mn_4O_9$ cathode material. A TG curve of a 1:1 stoichiometric mixture of $LiMnO_4{\cdot}3H_2O$ and $MnCO_3$ is shown in Fig. 1. The sample was heated to 450°C at a rate of 2°C/min in oxygen. The first weight loss is attributed to the loss of 3 moles of water beginning about 60°C. The second weight loss at ~150°C was caused by the decomposition of $LiMnO_4$

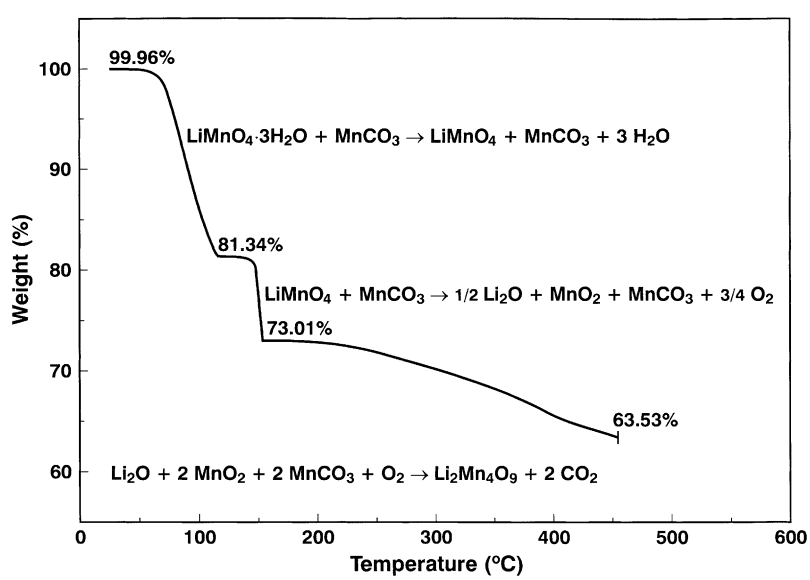

Fig. 1. TG curve of a $LiMnO_4 \cdot 3H_2O + MnCO_3$ mixture at a heating rate of 2°C/min in an oxygen atmosphere.

with the evolution of oxygen. This reaction is extremely exothermic, and slow heating rates and small sample sizes are required to preclude the expulsion of the sample from the TG boat. The final product forms during the third weight loss with the evolution of CO_2.

The proposed reactions for the three weight losses shown in Fig. 1 are given by Eqs. (1)–(3).

$$LiMnO_4 \cdot 3H_2O + MnCO_3 \rightarrow LiMnO_4 + MnCO_3 + 3H_2O \quad (1)$$

$$LiMnO_4 + MnCO_3 \rightarrow \tfrac{1}{2}Li_2O + MnO_2 + MnCO_3 + \tfrac{3}{4}O_2 \quad (2)$$

$$Li_2O + 2MnO_2 + 2MnCO_3 + O_2 \rightarrow Li_2Mn_4O_9 + 2CO_2 \quad (3)$$

Theoretical TG weight plateaus are calculated from the gravimetric factors determined from the molecular weights of the solid phases. The experimental TG plateau values are determined from the ratio of successive plateaus. Thus, the experimental TG values for the three reactions are 0.8137, 0.8976, 0.8702. These measured values are in excellent agreement with the theoretical values of 0.8167, 0.9003, and 0.8708. The measured weight plateau, 63.53%, for the overall reaction, Eq. (4), is in very good agreement with the theoretical value of 64.03%. The discrepancy is attributed to the simultaneous decomposition of the product at temperatures above about 400°C. At a heating rate of 2°C/min, the TG experiment lasted only about 220 min. It is emphasized, therefore, that much longer reaction times, as described later, are required for the preparation of the highly oxidized spinel material.

$$2LiMnO_4 \cdot 3H_2O + 2MnCO_3 \rightarrow Li_2Mn_4O_9 + 2CO_2 + 6H_2O + \tfrac{1}{2}O_2 \quad (4)$$

3.2. Determination of reaction temperature

The solid-state synthesis of the fully oxidized $Li_2Mn_4O_9$ phase is highly dependent on the calcination time and temperature. If the temperature is too low, it may not be possible to achieve a high degree of oxidation, even after several days of heating, because of the slower reaction kinetics. At higher temperatures, competition between the formation of the spinel and the reverse (decomposition) reaction can occur. This critical temperature dependence was investigated by TG analysis. An incompletely oxidized spinel was prepared by heating the precursors in a tube furnace at 400°C under oxygen. A portion of the material was transferred to the TG apparatus and heated at a slow rate of 1°C/min in oxygen starting at ~200°C. The TG behavior showed a steady increase in weight over the next 100 min as the spinel slowly oxidized. No further oxidation was observed between about 340 and 400°C. Above 400°C, the spinel material began to slowly lose oxygen as it decomposed back to $Li_2Mn_4O_8$. This temperature is in agreement with previously reported results [1] on the thermal stability of $Li_2Mn_4O_9$. However, this does not preclude decomposition of the spinel at lower temperatures provided sufficient calcination time is allowed. This was verified when we observed a decrease in the oxidation state of Mn in the spinel upon excessive heating at 365°C. Based on these initial TG results, we selected calcination temperatures in the range of 365–400°C for this study.

3.3. TG analysis

It has been reported [1] that $Li_2Mn_4O_9$ decomposes with a loss of oxygen when heated above 400°C for long periods of time, according to the following reaction:

$$Li_2Mn_4O_9 \rightarrow 2LiMn_2O_4 + \tfrac{1}{2}O_2 \quad (5)$$

At higher temperatures, the product of the above reaction, $LiMn_2O_4$, will decompose [12] according to the following reaction;

$$3LiMn_2O_4 \rightarrow 3LiMnO_2 + Mn_3O_4 + O_2 \quad (6)$$

The two-step thermal decomposition of "$Li_2Mn_4O_9$", shown by Eq. (5) and (6), was characterized by TG analysis [9] and by X-ray studies. Separable TG weight plateaus were established by selecting optimal experimental parameters such as small sample size, slow heating rate and inert atmosphere. The oxygen content of the starting material was then determined from the appropriate gravimetric factors and the measured plateau values.

TG curves of a commercial $LiMnO_4$ sample and our highly oxidized $Li_2Mn_4O_9$ material are shown in Fig. 2. The samples were heated at a rate of 10°C/min in an atmosphere of flowing helium. The weight plateau ratio (94.04/99.94) in curve (a) for the $LiMn_2O_4$ sample is in exact agreement with the theoretical value of 94.10% calculated from Eq. (6). The first weight loss for the highly oxidized material, curve (b), occurring from room temperature to about 300°C, is due to the evolution of adsorbed and combined water. The second weight loss, from about 300–600°C, is attributed to the decomposition of "$Li_2Mn_4O_9$" according to Eq. (5). The third weight loss, from about 600–800°C, is attributed to the decomposition of $LiMn_2O_4$ according to Eq. (6). Mn_3O_4 forms as a result of the decomposition of Mn_2O_3 at temperatures above 650°C in an inert atmosphere. The values of non-horizontal weight plateaus were determined from the minima in the TG derivative curves.

The oxygen content, z in $Li_2Mn_4O_{8+z}$, was determined by equating the molecular weights of the solid phases to the TG weight plateaus as follows:

$$Li_2Mn_4O_{8+z} \rightarrow 2LiMn_2O_4 + Z/2O_2 \quad (7)$$

$$\frac{2LiMn_2O_4}{Li_2Mn_4O_{8+z}} = \frac{361.6292}{361.6292 + 15.9994z} = \frac{95.17\%}{98.68\%} \quad z = 0.83$$

The final weight loss, attributed to the known decomposition reaction of $LiMn_2O_4$ (Eq. (6)), was used as a corroborative

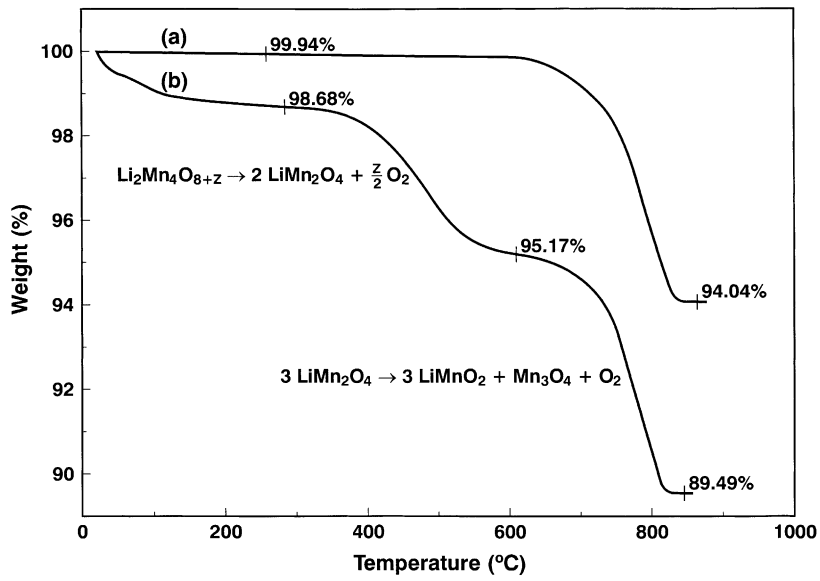

Fig. 2. TG curves of: (a) commercial $LiMn_2O_4$ cathode material; (b) highly oxidized $Li_2Mn_4O_{8+z}$ material at a heating rate of 10°C/min in a helium atmosphere.

measurement for the TG method. The theoretical plateau value, obtained from the ratio of the molecular weight of the products and reactants in Eq. (6), is 0.9410. As shown in Fig. 2, the experimental value, obtained from the ratio of the final plateaus (89.49%/95.17%), is 0.9403. This excellent agreement between the calculated and measured values provides strong evidence for the validity of the TG method for determining the oxygen content in the nominal compound $Li_2Mn_4O_{8+z}$. Implicit in the TG method is the assumption that the material is single phase and the atomic ratio of Mn to Li in the spinel phase is indeed 2. The method can be used for other Mn/Li ratios by adjusting the Li and Mn subscripts in Eq. (7). If the material is not single phase, then TG analysis will show significant deviations from the theoretical value of 0.9410. The phase purity of the spinels was confirmed by XRD analysis. In highly oxidized spinels, such as sample 6, there was also very good agreement between the TG analysis and the chemical analysis, as discussed in a later section.

3.4. Derivative thermogravimetry (DTG)

DTG can provide important insights into the thermal behavior of materials that are not readily apparent from inspection of the parent TG curve. For example, highly asymmetric or split peaks may be indicative of complex decomposition mechanisms or the presence of extraneous phases. Such phases are usually undetectable by XRD because of the extreme similarity of the manganese spinel XRD patterns. DTG curves of highly oxidized $Li_2Mn_4O_{8+z}$ phases revealed symmetric derivative peaks in the temperature range 300–600°C. Poorly oxidized material, on the other hand, displayed asymmetric peaks or a prominent shoulder at 410°C. This can be caused by the simultaneous decomposition of the unreacted $MnCO_3$ precursor. The evolution of CO_2 was detected by simultaneous TG/FTIR measurements using samples that had large DTG peak shoulders. In general, we found that CO_2 evolution correlated with the peak at 410°C. This is virtually identical to the observed DTG decomposition peak temperature of our $MnCO_3$ precursor material. A highly oxidized "$Li_2Mn_4O_9$" material, having a symmetric DTG curve, showed no evidence of CO_2 evolution.

3.5. X-ray diffraction

Spinel materials, described later in Table 1, were prepared in oxygen by heating precursor mixtures for 20, 40 and 60 h at 365 and 400°C. A typical XRD powder pattern for sample 5C, heated for 122 h is shown in Fig. 3. The XRD data indicated that only a single phase was present. As cited by Xia and Yoshio [8], however, small amounts of impurities are difficult to distinguish by XRD. The lattice parameter for sample 5B, which is equivalent to $Li_{1.97}Mn_{4.00}O_{8.54}$, was determined to be 8.142 Å. The oxidation state of manganese in this sample was determined by potentiometric titration to be +3.816. These results are in excellent agreement with the values of 8.146 Å and +3.79 reported by Masquelier et al. [7]. Similar lattice parameters of 8.143 [4], 8.137 [6], and 8.150 Å [8] have been reported for highly oxidized spinels. Other investigators, however, have reported much larger lattice parameters of 8.174 [1,6] and 8.162 Å [2] for "$Li_2Mn_4O_9$". It is well known [7] that the lattice parameter decreases with increasing manganese oxidation state. Since attempts to prepare fully oxidized $Li_2Mn_4O_9$ have never been demonstrated, we believe these materials have lattice parameters more in agreement with manganospinels having lower oxidation states.

Table 1
Chemical analysis of lithium manganospinels[a]

Sample	T (°C)	Time (h)	%Li	%Mn^{4+}	%Mn^{3+}	m	x	y	Spinel Composition $Li_{1-x}Mn_{2-y}O_4$	z In nominal $Li_2Mn_4O_{8+z}$
A. Oxygen-rich										
1A	400	17	3.70	38.66	19.12	3.669	0.029	0.084	$[Li_{0.971}\square_{0.29}]_{8a}[Mn_{1.916}\square_{0.84}]_{16d}O_4$	0.35
1B	400	17	3.70	40.90	16.38	3.714	0.032	0.107	$[Li_{0.968}\square_{0.32}]_{8a}[Mn_{1.893}\square_{0.107}]_{16d}O_4$	0.45
1C	400	17	3.70	41.27	16.52	3.714	0.042	0.104	$[Li_{0.958}\square_{0.042}]_{8a}[Mn_{1.896}\square_{0.104}]_{16d}O_4$	0.44
3A	390	21	3.73	43.17	15.23	3.739	0.047	0.115	$[Li_{0.953}\square_{0.047}]_{8a}[Mn_{1.885}\square_{0.115}]_{16d}O_4$	0.49
4A	390	39	3.73	44.13	13.63	3.764	0.046	0.128	$[Li_{0.9954}\square_{0.046}]_{8a}[Mn_{1.872}\square_{0.128}]_{16d}O_4$	0.55
4B	390	48	3.75	45.29	12.23	3.788	0.041	0.141	$[Li_{0.959}\square_{0.041}]_{8a}[Mn_{1.859}\square_{0.141}]_{16d}O_4$	0.61
5A	365	41	3.60	45.05	13.36	3.770	0.083	0.121	$[Li_{0.917}\square_{0.083}]_{8a}[Mn_{1.879}\square_{0.121}]_{16d}O_4$	0.52
5B	365	67	3.60	47.25	10.63	3.816	0.086	0.143	$[Li_{0.914}\square_{0.086}]_{8a}[Mn_{1.857}\square_{0.143}]_{16d}O_4$	0.62
5C	365	122	3.63	45.84	13.02	3.778	0.077	0.127	$[Li_{0.923}\square_{0.077}]_{8a}[Mn_{1.873}\square_{0.127}]_{16d}O_4$	0.54
6A	365	40	3.76	50.25	7.18	3.876	0.057	0.179	$[Li_{0.943}\square_{0.057}]_{8a}[Mn_{1.821}\square_{0.179}]_{16d}O_4$	0.79
6B	365	117	–	–	–	3.91	–	–	–	0.85
6C	365	165	3.69	52.89	4.38	3.924	0.08	0.20	$[Li_{0.92}\square_{0.080}]_{8a}[Mn_{1.80}\square_{0.20}]_{16d}O_4$	0.88
B. Lithium-rich									$[Li_{1+x}Mn_{2-y}O_4$	
2	400	70	3.84	43.41	12.53	3.776	0.10	0.14	$[Li]_{8a}[Mn_{1.85}\square_{0.014}Li_{0.01}]_{16d}O_4$	0.62

[a] Where m is average oxidation state of Mn and z shows the extent of oxidation of nominal $Li_2Mn_4O_{8+z}$. Samples were prepared under flowing oxygen except sample 1A, which was heated in air, and sample 1C, which was heated under ozone. Sample 2 was prepared using a combination of flowing oxygen and 30% H_2O_2. Samples 3, 4, 5 were intermittently ground. Samples 6 were prepared using anhydrous $LiMnO_4$. Sample 6B was analyzed by TG.

3.6. Chemical analysis

Chemical analyses were performed on samples prepared under a variety of conditions. Some representative analysis data are shown in Table 1. The chemical analysis provides data for determining the total manganese oxides present, and the average oxidation state of the manganese. The efficacy of the analytical procedure was confirmed by determining the total percent manganese oxides in $Li_2Mn_4O_9$ ($Li_2O{\cdot}4MnO_2$), wherein the theoretical value is 92.09% when all of the manganese is in the +4 oxidation state.

Although stoichiometric precursor mixtures were used, most of the spinel products were found to have a Li/Mn ratio slightly greater than the intended 1:2 ratio. This observation has also been reported by others [4,7]. We attributed this to some residual water in the $MnCO_3$. Furthermore, the presence of unreacted $MnCO_3$ could adversely affect the analysis. When a known amount of $MnCO_3$ was added to pre-analyzed commercial $LiMnO_4$, the Mn^{4+}/Mn^{3+} ratio was dramatically reduced. This was not observed during analyses of spinels that were synthesized under appropriate conditions, further confirming the TG-FTIR data that the $MnCO_3$ had reacted completely.

Although the $Li_2Mn_4O_{8+z}$ notation implies an "oxygemroch" spinel, a positive value of z implies overall cation deficiency, such as $Li_{1-x}Mn_{2-y}O_4$. For these "oxygen-rich"

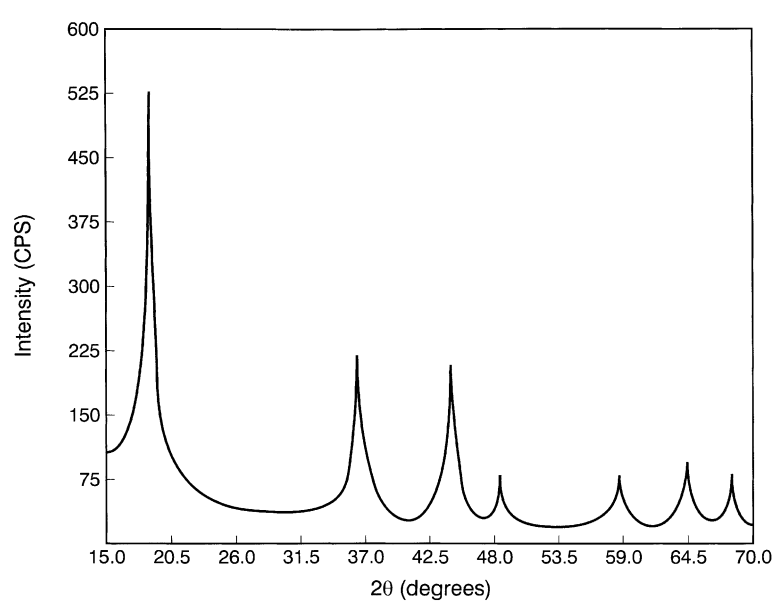

Fig. 3. X-ray diffraction pattern of oxidized spinel, sample 5C.

spinels, the values of x and y in Table 1, represent the vacancies in the tetrahedral (8a) and octahedral (16d) sites respectively, for a $Li_{8a}[Mn]_{16d}O_4$ spinel. For a unit cell $LiMn_2O_4$, the number of total tetrahedral sites (lithium plus vacancies) is 1, and the total octahedral sites (Mn plus vacancies) is 2. We can calculate the values of x and y from valance balance. When the ratio of Li/Mn in a compound containing 1 mole Mn is n, and the average oxidation state of Mn is m, a spinel of composition $Li_{2n}Mn_2O_{n+m}$ has 8a vacancy sites, x, given by $1-8n/(n+m)$ and 16d vacancies, y, given by $2-8/(n+m)$. A value of z, which shows the extent of oxidation of a spinel of nominal composition $Li_2Mn_4O_{8+z}$, was calculated from the ratio of Li/Mn in which the concentration of Mn was normalized to 4 moles in the spinel composition.

3.7. Oxidizing environment

To determine the effects of different oxidizing environments, the synthesis was performed at 400°C for 17 h in air, oxygen, and in an ozone-oxygen atmosphere. Some samples were further treated with 30% hydrogen peroxide. The data for samples 1A (air), 1B (O_2) and 1C (mix of O_2 and ozone) in Table 1 show that oxygen was more effective than air in producing an oxygen-rich spinel. Ozone had no beneficial effect on the extent of oxidation of the product.

A lithium-rich spinel (sample 2) was produced when precursors were heated under oxygen for 70 h and then heated an additional 18 h with excess 30% hydrogen peroxide. Heating the sample for another 44 h with peroxide produced no additional oxidation. Based on these results, we selected oxygen as the optimal oxidizing atmosphere.

3.8. Effect of grinding the sample

The effect of numerous intermittent grinding procedures during synthesis of the spinel was investigated. These syntheses were conducted at 390°C since higher temperatures appeared to be detrimental to forming the highly oxidized spinel. The analytical results for sample (3A), heated for 21 h, are shown in Table 1. Analysis showed that the oxidation state of Mn progressively increased through 36 h of heating, achieving a value of +3.744. After the next sample was taken at 51 h, the oxidation state of Mn had decreased. Samples heated for <4 h displayed the multi-peak DTG behavior discussed earlier, with a dominant $MnCO_3$ peak at ~410°C. As the grinding and heating procedure progressed to 8 h and beyond, smoother DTG curves were observed. The procedure was repeated using a similar precursor mixture. The products were analyzed after calcination for 20, 27, 39 (sample 4A), and 48 (sample 4B) and 60 h. The oxidation state of Mn was observed to reach a maximum after 48 h. With these precursors, the best results required approximately 48 h calcination at 390°C. The preparation of these materials in a reproducible manner is far from trivial, requiring careful selection of the precursors and the calcination temperature and time.

3.9. Effect of lower synthesis temperature

For our small (~3 g) samples, the decomposition of the product, represented by k_d, began to exceed the rate of formation of the spinel, k_f, after ~48 h at 390°C. This is illustrated by the competing reactions of the synthesis.

$$2LiMnO_4 + 2MnCO_3 \xrightarrow{k_f} Li_2O + 2MnO_2 + 2MnCO_3 + 1.5O_2$$
$$\xrightarrow{1/2O_2} Li_2Mn_4O_9 + 2CO_2 \xrightarrow{k_d} 2LiMn_2O_4 + \tfrac{1}{2}O_2 + 2CO_2$$

To decrease the rate of the reverse (decomposition) reaction, the synthesis procedure was carried out at 365°C. After intervals of 21, 41, 67, 94, and 122 h of intermittent grinding and heating at 365°C, the average oxidation state of Mn was 3.70, 3.70, 3.816, 3.782 and 3.778, respectively. Thus, it is clear that a maximum in the Mn oxidation state occurs despite the lower reaction temperature. The analytical data for 41, 67 and 122 h (samples 5A–5C), are shown in Table 1. Table 1 shows that the average Mn oxidation state was higher in the material synthesized at 365°C than in the 390°C material although more time was required at 365°C to achieve a highly oxidized material. Analysis showed the oxidation state of Mn increased with decreasing reaction temperatures, from 400 to 390–365°C.

3.10. Adsorption of water by spinels

TG analysis showed that spinel materials picked up atmospheric moisture to different degrees. Whereas TG curves showed that $LiMn_2O_4$ ($Li_2Mn_4O_8$) samples were completely anhydrous (Fig. 2a), spinels in which the value of $z > 0$ had a propensity to adsorb atmospheric moisture. As shown in Fig. 2b, the highly oxidized spinel material contains a considerable amount of adsorbed and combined water that is evolved from room temperature to about 250°C.

3.11. Effect of water of hydration

The effect of the permanganate water of hydration was examined. As shown in Table 1 spinels prepared from the anhydrous permanganate (6A–6C) were more highly oxidized than those prepared from the hydrated precursor (5A–5C) when prepared under identical conditions. Compare 5A with 6A and 5C with 6B. The composition of sample 6B was not determined by chemical analysis. Instead, the oxygen content of sample 6B was determined by TG to be $z = 0.85$. From this result, and assuming a Li/Mn ratio of 1:2, the oxidation state of Mn, m, was calculated to be 3.91. These TG results are in very good agreement with the chemical analysis data for samples 6A and 6C.

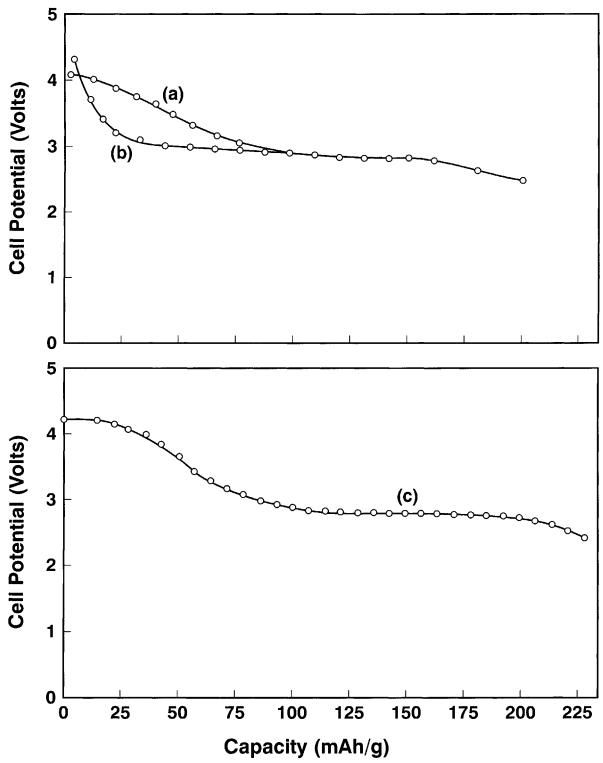

Fig. 4. Discharge behavior of $Li_2Mn_4O_{8+z}$ cathode material: (a) 4th cycle; (b) 8th cycle of sample 4B at 0.1 mA/cm^2 in 1 M $LiAsF_6$/PC; (c) 1st cycle of sample 6C at 1.5 mA/cm^2 in 1 M $LiPF_6$ in EC/EMC.

3.12. Electrochemistry

The electrochemical performance of several spinel materials samples 4B, 5C, 6C, and commercial $LiMn_2O_4$, was evaluated as cathodes in prismatic laboratory cells. The cycling performance of sample 4B was evaluated using 1 M $LiAsF_6$/PC electrolyte. During the initial cycling, the discharge curves did not show any sharp voltage transition as might be expected for a low crystalline defect spinel. The initial discharge revealed a small 4 V plateau with a gradual transition into a 3 V plateau. The initial capacity of the fourth cycle is shown in Fig. 4a. The discharge curve, shown in Fig. 4b, that occurs after eight shallow cycles at 0.1 mA/cm^2 displays primarily a 3.0 V plateau.

The cycling behavior was evaluated using 1 M LiP_6 EC/EMC electrolyte in order to increase the rate capability. Samples 5C and 6C were cycled between 4.5 and 2.5 V at 1.5 mA/cm^2. Very little initial charge acceptance was observed in sample 6C because of the high oxidation state of Mn in the spinel. This highly oxidized spinel now gives rise to two voltage plateaus. The initial discharge capacity of sample 6C, shown in Fig. 4c, exceeded the 213 mAh/g expected for a 3-faraday reduction. Upon replacing the lithium, separator and electrolyte after 10 cycles, an 8% increase in capacity was observed, indicating components other than the cathode contributed to some loss of capacity upon cycling.

In general, both the commercial $LiMn_2O_4$ and our spinel cathodes gave poor cycling performance in the prismatic cells. This loss of capacity was attributed to poor electrode compression. Thus, the cycling behavior of a cathode prepared from sample 5C was compared with a similarly prepared $LiMn_2O_4$ cathode in coin cells, using a lithium anode and EC–DMC–DEC electrolyte. The cells delivered 9 cycles before the lithium anode began to short each cell. In contrast to the $LiMn_2O_4$ cathode, however, the cathode prepared from sample 5C retained capacity over the first few cycles. As shown in Fig. 5, the cathode made from sample 5C provided excellent total capacity relative to the $LiMn_2O_4$ cathode.

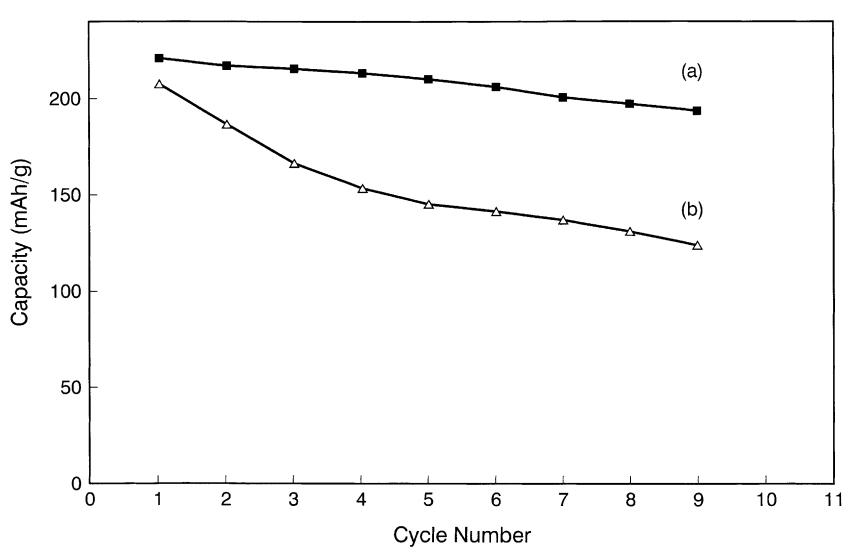

Fig. 5. Comparison of capacity retention of spinel cathode materials in coin cells: (a) Sample 5C; (b) $LiMnO_4$.

4. Conclusion

Highly oxidized $Li_2Mn_4O_9$ defect spinel materials have been prepared from $LiMnO_4$ and $MnCO_3$ precursors. A maximum z value of 0.88 in $Li_2Mn_4O_{8+z}$ was obtained. We developed a TGA method of analyzing the spinel material that is in excellent agreement with chemical analysis. The materials were characterized using chemical, TG and XRD analyses. Electrochemical discharge proved to have excellent capacity (>200 mAh/g) and capacity retention relative to $LiMn_2O_4$ when single cells were cycled from 4.5 to 2.5 V in coin cells.

Acknowledgements

We gratefully acknowledge the assistance of Dr. Eric Wuchina and Dr. James Zaykoski for the X-ray analyses. We wish to thank the NSWC In-House Laboratory Independent Research (ILIR) program for funding support.

References

[1] A. de Kock, M.H. Rossouw, L.A. de Picciotto, M.M. Thackeray, W.I.F. David, I.M. Ibberson, Mater. Res. Bull. 25 (1990) 657.
[2] M.M. Thackeray, A. de Kock, M.H. Rossouw, D. Liles, R. Bittihn, D. Hoge, J. Electrochem. Soc. 139 (1992) 363.
[3] M.M. Thackeray, M.H. Rossouw, J. Solid State Chem. 113 (1994) 441.
[4] M.M. Thackeray, A. de Kock, W.I. David, Mat. Res. Bull. 28 (1993) 1041.
[5] M.M. Thackeray, M.H. Rossouw, J. Solid State Chem. 113 (1994) 441.
[6] R.J. Gummow, A. de Kock, M.M. Thackeray, Solid State Ionics 69 (1994) 59.
[7] C. Masquelier, M. Tabuchi, K. Ado, R. Kanno, Y. Kobayashi, Y. Maki, O. Nakamura, J.B. Goodenough, J. Solid State Chem. 123 (1996) 255.
[8] Y. Xia, M. Yoshio, J. Electrochem. Soc. 144 (1997) 4186.
[9] S. Dallek, in: Proceedings of the 38th Power Sources Conference, 1998, p. 378.
[10] C. Mueller, P. Smith, W. Kilroy, in: Proceedings of the 1st Hawaii Lithium Battery Conference.
[11] F. Leroux, D. Guyomard, Y. Piffard, Solid State Ionics 80 (1995) 299.
[12] J. Tarascon, W. Mckinnon, F. Coowar, T. Bowmer, G. Amatucci, D. Guyomard, J. Electrochem. Soc. 141 (1994) 1421.